J Neurophysiol 92: 2510–2519, 2004.
First published June 2, 2004; 10.1152/jn.00108.2004.

How Retinal Ganglion Cells Prevent Synaptic Noise From Reaching the Spike Output

Jonathan B. Demb,[1,2,3] Peter Sterling,[1] and Michael A. Freed[1]

[1]*Department of Neuroscience, University of Pennsylvania, Philadelphia, Pennsylvania 19104; Departments of* [2]*Ophthalmology and Visual Sciences and* [3]*Molecular, Cellular and Developmental Biology, University of Michigan, Ann Arbor, Michigan 48105*

Submitted 3 February 2004; accepted in final form 25 May 2004

Demb, Jonathan B., Peter Sterling, and Michael A. Freed. How retinal ganglion cells prevent synaptic noise from reaching the spike output. *J Neurophysiol* 92: 2510–2519, 2004. First published June 2, 2004; 10.1152/jn.00108.2004. Synaptic vesicles are released stochastically, and therefore stimuli that increase a neuron's synaptic input might increase noise at its spike output. Indeed this appears true for neurons in primary visual cortex, where spike output variability increases with stimulus contrast. But in retinal ganglion cells, although intracellular recordings (with spikes blocked) showed that stronger stimuli increase membrane fluctuations, extracellular recordings showed that noise at the spike output is constant. Here we show that these seemingly paradoxical findings occur in the same cell and explain why. We made intracellular recordings from ganglion cells, in vitro, and presented periodic stimuli of various contrasts. For each stimulus cycle, we measured the response at the stimulus frequency (F1) for both membrane potential and spikes as well as the spike rate. The membrane and spike F1 response increased with contrast, but noise (SD) in the F1 responses and the spike rate was constant. We also measured membrane fluctuations (with spikes blocked) during the response depolarization and found that they did increase with contrast. However, increases in fluctuation amplitude were small relative to the depolarization (<10% at high contrast). A model based on estimated synaptic convergence, release rates, and membrane properties accounted for the relative magnitudes of fluctuations and depolarization. Furthermore, a cell's peak spike response preceded the peak depolarization, and therefore fluctuation amplitude peaked as the spike response declined. We conclude that two extremely general properties of a neuron, synaptic convergence and spike generation, combine to minimize the effects of membrane fluctuations on spiking.

INTRODUCTION

Synaptic vesicles are released stochastically, and because of this a stimulus that releases more vesicles at a neuron's input might increase noise at its spike output. Indeed, as a signal intensifies for neurons in primary visual cortex, noise (SD) in the spike output rises (Dean 1981; Schiller et al. 1976; Tolhurst et al. 1981, 1983). But for retinal ganglion cells, noise at the spike output is constant. This has been found by extracellular recordings from various cell types, including X and Y cells in cat (Reich et al. 1997; Sestokas and Lehmkuhle 1988; but see Levine et al. 1992, 1996) and M and P cells in monkey (Croner et al. 1993; Rüttiger et al. 2002; Sun et al. 2004). Thus there appears to be a general principle: the retinal output to the brain behaves like a pure signal with added noise that is independent of the input level. Consequently, early vision can improve proportionally with response level.

Intracellular recordings show quite different behavior for the ganglion cell's membrane voltage. As depolarization rises with stimulus intensity, the voltage noise (fluctuation amplitude) increases in proportion to the square root of the depolarization. This has been found for X and Y cells (Freed 2000a,b) and also for second-order visual neurons in the fly (Laughlin et al. 1987). The rise in fluctuations with the signal has been attributed to Poisson statistics of excitatory presynaptic release (Freed 2000a; Freed et al. 2003; Laughlin and Sejnowski 2003; Laughlin et al. 1987). The two sets of apparently contradictory observations were made with different methods and different stimuli (extracellular: sinusoidal modulation; intracellular: square-wave modulation), so we wondered if they could be observed in the same cell under the same conditions, and if so, what might prevent a ganglion cell's variable level of input noise from appearing in the spike output?

To investigate this we made intracellular recordings from mammalian ganglion cells in vitro, which allowed both the graded membrane potential (V_m) and the spike responses to be analyzed in the same cell. We presented periodic stimuli at various contrasts, similar to those used in vivo (Croner et al. 1993; Rüttiger et al. 2002; Sun et al. 2004). We then constructed a simple model that reproduced the key properties of the V_m response that showed that summing numerous small events reduces the amplitude of fluctuations relative to the amplitude of depolarization. Of course, such signal averaging is well known; yet precisely how it serves the ganglion cell was not known. And the result raises the further question why do cortical neurons not remove their input noise in the same way?

METHODS

Intracellular recording

From a guinea pig anesthetized with ketamine (100 mg/kg), xylazine (20 mg/kg), and pentobarbital (150 mg/kg), both eyes were removed after which the animal was killed by anesthetic overdose (in accordance with University of Pennsylvania and National Institutes of Health guidelines). The whole retina attached to the pigment epithelium, choroid, and sclera was mounted flat in a chamber on a microscope stage as described previously (Demb et al. 1999). Retina was superfused (~4 ml/min) with oxygenated (95% O-5% CO_2) Ames medium (Sigma, St. Louis, MO) at 32–36°C. Acridine orange (0.001%; Molecular Probes, Eugene, OR) was added to the superfusate, allowing ganglion cell somas to be identified by fluorescence during brief exposure to UV light. A glass electrode (tip resistance: 80–200 MΩ), filled with 1% pyranine (Molecular Probes) in 2 M

Address for reprint requests and other correspondence: J. B. Demb, University of Michigan, Kellogg Eye Center, 1000 Wall St., Ann Arbor, Michigan 48105 (E-mail: jdemb@umich.edu).

The costs of publication of this article were defrayed in part by the payment of page charges. The article must therefore be hereby marked "*advertisement*" in accordance with 18 U.S.C. Section 1734 solely to indicate this fact.

potassium acetate, was used to penetrate somas in the visual streak. Tetrodotoxin (TTX) was purchased from Sigma, and lidocaine *N*-ethyl bromide (QX-314) was purchased from Research Biochemicals (Natick, MA).

Membrane potential (V_m) was amplified, continuously sampled at 2–5 kHz, and stored on computer as previously described (Demb et al. 1999). Programs were written in Matlab (Mathworks, Natick, MA) to analyze responses separately in the spike rate and subthreshold V_m. Spikes were detected off-line (Zaghloul et al. 2003). V_m was analyzed after removing spikes computationally: we performed a linear interpolation of V_m between 1 ms before and 1–4 ms after each spike (Fig. 1). To remove high-frequency noise, membrane responses were low-pass filtered by convolving with a Gaussian (SD = 3 ms or 106 Hz). The resting potential was determined by averaging the potential before and after a stimulus. In some recordings, current was injected through the pipette. In these cases, V_m was corrected for unbalanced electrode resistance as described previously (Zaghloul et al. 2003).

Visual stimulation

The stimulus was displayed on a miniature monochrome computer monitor (Lucivid MR1-103, Microbrightfield, Colchester, VT) projected through the top port of the microscope through a ×2.5 objective and focused on the photoreceptors (mean luminance = ~10^5 isomerizations cone^{-1} s^{-1}; resolution = 852 × 480 pixels; 60-Hz vertical refresh). The relationship between gun voltage and monitor intensity was linearized in software with a lookup table. Stimuli were defined by percent Michelson contrast: $100 \times (I_{max} - I_{min})/(I_{max} + I_{min})$, where I_{max} and I_{min} are the peak and trough intensities (range = 0–100%). Stimuli were programmed in Matlab using extensions provided by the high-level Psychophysics Toolbox (Brainard 1997) and the low-level Video Toolbox (Pelli 1997).

Contrast response functions

A cell was stimulated with a sinusoidally modulated spot (0.5 mm diam) over the receptive field center or a drifting sine-wave grating (spatial frequency, 0.5–2.2 cycles/mm). The stimulus modulated or drifted at between 2 and 7.5 Hz, for 8–200 cycles. The main findings were not affected by stimulus type, temporal frequency, or number of cycles and were similar between cell type (on or off center), and so data have been combined for population analyses. A cell typically showed an initial response (1st 1–2 s) that was elevated by ~20% relative to subsequent responses, which showed a steady average response; thus the first 1–2 s of response were discarded, and the variability was computed on the subsequent response. The membrane and spike responses were both analyzed with 1-kHz sampling. The spike train was thus defined as a rate in 1-ms bins.

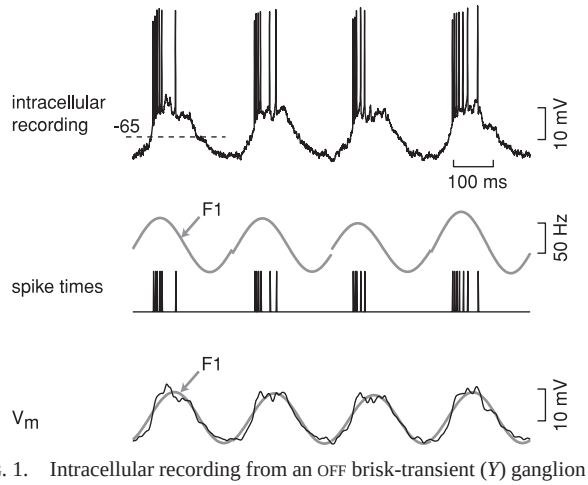

FIG. 1. Intracellular recording from an OFF brisk-transient (*Y*) ganglion cell. A spot was modulated at 4 Hz covering the dendritic field (0.5 mm diam, 90% contrast). The response was separated into a train of spike times and a graded membrane potential (V_m). A Fourier transform was performed on each response cycle for spikes and V_m; the response at the stimulus frequency (F1 component) is shown as a gray line above the spike train or superimposed on the V_m. The cell rested at −65 mV with a maintained 2-Hz discharge.

Response magnitude was calculated for each stimulus cycle (Croner et al. 1993; Reich et al. 1997). Fourier analysis was performed on each cycle of V_m or spike responses to quantify the amplitude and phase at the fundamental frequency (F1). The mean ± SD across cycles was calculated either on the amplitudes alone or in the complex plane on both amplitude and phase (i.e., vector mean and SD) (Croner et al. 1993). For spikes, the response was also quantified, independent of Fourier analysis, as the number of spikes per cycle. This measure is easier to interpret in OFF cells, which had a relatively low maintained discharge; thus the response on each cycle resembled a "burst" of spikes that could be quantified by measuring rate. For all measures, contrast response functions were fit with a function, whose parameters were obtained by least-squares fits using standard routines in Matlab.

Measure of V_m fluctuations

In some cells, V_m was measured in the absence of spiking either by blocking sodium channels (TTX, QX-314) or by injecting negative current (see following text). Contrast-dependent changes in the response typically appeared in the first four to nine harmonics of the stimulus frequency. Thus to derive membrane fluctuations, we calculated the Fourier transform of V_m response across cycles, removed the mean and first 10 harmonics of stimulus modulation, and then performed an inverse Fourier transform; this resulted in "fluctuation" traces (Fig. 3). This procedure removed the stimulus-driven component from responses to contrasts >0% but did not significantly affect the response to 0% contrast (resting potential; Fig. 3). The average cycle fluctuation amplitude was the SD of the fluctuation traces across cycles, and this was computed at 1 kHz (Fig. 3). We smoothed the fluctuation amplitude trace by squaring each value (variance), smoothing with a 50-ms moving window, and taking the square-root (SD; Fig. 3). To measure changes in fluctuation amplitude during the "peak" response (Fig. 4*A*), we calculated the mean difference in variance between the peak response (50-ms period) and the resting potential, and then took the square root (SD); a similar procedure was used to measure change in fluctuation amplitude during the "trough" response (Fig. 4*B*).

Simulation

A ganglion cell's V_m was simulated in Matlab as the sum of multiple bipolar cell inputs. Each input provided a train of excitatory postsynaptic potentials (EPSPs), according to Poisson statistics; that is, the average rate was controlled, but individual EPSP timings were random. In *test 1*, the EPSP was a decreasing exponential with a peak amplitude of 0.1 mV and a time constant (τ) of 10 ms. Actual measurements in cat Y cells suggest an amplitude of ~0.04 mV and τ of ~10 ms (Freed 2000a). *Test 1* summed 1,000 bipolar synapses. Y cells of the size studied here (dendritic field diameter: ~0.5 mm) (Demb et al. 2001a) receive ≥1,000 bipolar synapses studied in cat by electron microscopy (Freed 2000a; Freed and Sterling 1988; Kier et al. 1995), and we have confirmed this in guinea pig by immunostaining for synaptic ribbons (P. Sterling, unpublished observations). The basal rate was 4 EPSPs synapse^{-1} s^{-1}. Measurements suggest that basal release at steady photopic luminance is ≥2 vesicles synapse^{-1} s^{-1} (Freed 2000a). Stimulus-evoked responses were simulated by adding a sinusoidally modulated EPSP rate around the basal rate, and this was performed for 50 stimulus cycles per modulation amplitude. The modulation amplitude ranged from 1 to 4 EPSPs synapse^{-1} s^{-1}; thus the maximum amplitude equaled the basal release rate, and the response ranged from zero to twice the basal rate. Real cells showed a saturating response at high contrast (see following text), and thus

modulation amplitude in the simulation does not translate linearly to contrast.

In addition to *test 1*, which set parameter values to previous measurements, we display two alternatives, the effect of reducing the basal release rate to 0 EPSPs synapse^{-1} s^{-1} (*test 2*), and additionally reducing the number of synapses by 10-fold (from 1,000 to 100; *test 3*). To maintain a constant mean voltage signal in *test 3*, the EPSP amplitude was increased by 10-fold (from 0.1 to 1 mV). We also tested basal rates of 1 or 2 EPSPs synapse^{-1} s^{-1} and $\tau = 5$ or 20 ms. We also tried reducing the number of synapses to 10, but then the raw trace resembled a series of individual EPSPs rather than a typical intracellular recording.

A model's average cycle response and fluctuation amplitude could be calculated directly (Campbell's theorem) (Katz and Miledi 1972; Rice 1944; Segal et al. 1985). The voltage response for steady (unmodulated) Poisson release was calculated as

$$V = na\tau$$

where V is voltage, n is the rate of EPSPs (number of synapses $\times$ quantal rate synapse^{-1}), and a and τ are the amplitude and time constant of the EPSP ($a\tau$ is the integral of the EPSP). The time-varying voltage response with a modulated rate was calculated as

$$V(t) = n(t) * ae^{-t/\tau}$$

where t is time, and * represents convolution.

Given the rate of Poisson release, the variance of the voltage response for steady (unmodulated) release could be calculated as

$$\sigma^2 = (na^2\tau)/2$$

where σ^2 represents variance, and 1/2 is a shape factor related to the exponential nature of the EPSP (Katz and Miledi 1972; Rice 1944; Segal et al. 1985). We calculated the time-varying σ^2 with a modulated rate as

$$\sigma(t)^2 = n(t) * (ae^{-t/\tau})^2$$

and calculated membrane fluctuation amplitude by taking the square root, σ(t).

RESULTS

Basic response properties

We recorded from brisk-transient (Y) ganglion cells (5 on center and 21 off center). Resting potentials were -62.5 ± 1.3 (SE) mV and maintained discharges were 8.1 ± 1.7 spikes/s ($n = 22$). Maintained discharge was lower in OFF cells (4.9 ± 0.8 spikes/s) than in ON cells (19.0 ± 4.0 spikes/s) as reported in vivo (Troy and Robson 1992). Our cells were identified visually by their large somas (20–25 μm diam) and functionally by multiple criteria: a brisk-transient response to a contrast step; a "center/surround" receptive field, with opposite responses to a spot (diameter, 500 μm) versus an annulus (inner/outer diameter, 740/2,000 μm); and a frequency-doubled response to a contrast-reversing grating (spatial frequency, 4.3 cycles/mm) (Demb et al. 2001a,b; Enroth-Cugell and Robson 1966; Hochstein and Shapley 1976; Peichl et al. 1987).

Contrast response functions

We measured the signal and noise of ganglion cells at multiple response levels by varying stimulus contrast. Thus we could compare quantitatively the contrast-response function of the membrane potential (V_m) and spike response, and we could compare the in vitro spike response to previous measurements in vivo. A cell was stimulated with a sinusoidally modulated spot over the receptive field center or a drifting sine-wave grating (see METHODS). For each stimulus cycle, the intracellular response was separated into two signals, the subthreshold V_m and the spike times (Fig. 1; see METHODS). For each cycle of spikes, we calculated the amplitude and phase of the fundamental frequency (F1) as well as the spike rate (see METHODS). For each cycle of V_m, we calculated the amplitude and phase of F1.

For all cells, the spike and V_m responses increased with contrast (Fig. 2*A*). Data were fit with the descriptive function (Hill's equation) (Naka and Rushton 1966)

$$r = a(c^p/[c^p + \sigma^p])$$

where r is response, c is contrast, and a, σ, and p are free parameters. We used the fit to calculate a half-saturation value: the contrast that elicited a half-maximal fitted response. The spike F1 response showed half-saturation at $29 \pm 2.3\%$ contrast; the V_m F1 response showed half-saturation at $27 \pm 2.2\%$. The half-saturation of V_m and spikes was correlated ($r = 0.75$, $n = 22$ cells, $P < 0.001$), suggesting that the saturation of the spiking response relates directly to the saturation of the V_m response (Fig. 2*B*).

The average spike rate, measured across the full stimulus cycle, increased from 0 to 100% contrast, and this increase was larger in OFF cells (12.5 ± 1.2 spikes/s, $n = 17$) relative to ON cells (5.8 ± 2.4 spikes/s, $n = 5$). The spike rate increases with contrast when there is a large F1 amplitude relative to the maintained discharge; this is a simple result of the rectification of the spike threshold (i.e., response modulations can increase above the mean rate more than they can decrease below the mean rate). In OFF cells, the maximum F1 amplitude was large (30.1 ± 2.2 spikes/s) relative to the maintained discharge (4.9 ± 0.8 spikes/s), whereas for ON cells, the maximum F1 amplitude (23.3 ± 4.1 spikes/s) was similar to the maintained discharge (19.0 ± 4.0 spikes/s). The maintained discharge and maximum F1 amplitudes were similar to those measured in vivo (Croner et al. 1993; Troy and Robson 1992).

Noise in the modulated response of V_m and spikes was independent of contrast

We measured the noise (SD) of the modulated response at each contrast. For spikes, noise was measured as the SD of F1 computed either on the amplitudes ($SD_{spike\ F1}$) or in the complex plane based on both amplitude and phase ($SD_{spike\ F1,\ complex}$) (Croner et al. 1993); the $SD_{spike\ F1,\ complex}$ can be directly compared with in vivo measurements. We also calculated the noise in the spike rate ($SD_{spike\ rate}$), measured across the full stimulus cycle. In all cases, noise appeared to be constant with contrast (Fig. 2*A*). The average $SD_{spike\ F1,\ complex}$ was 5.0 ± 0.5 spikes/s, similar to the value measured in vivo (Croner et al. 1993; Reich et al. 1997; Rüttiger et al. 2002; Sun et al. 2004).

The effect of contrast on noise was quantified by fitting the noise values with a regression line. If noise was independent of contrast, the regression slope would be zero. On average, the slopes of $SD_{spike\ F1,\ complex}$ and $SD_{spike\ rate}$ were not different

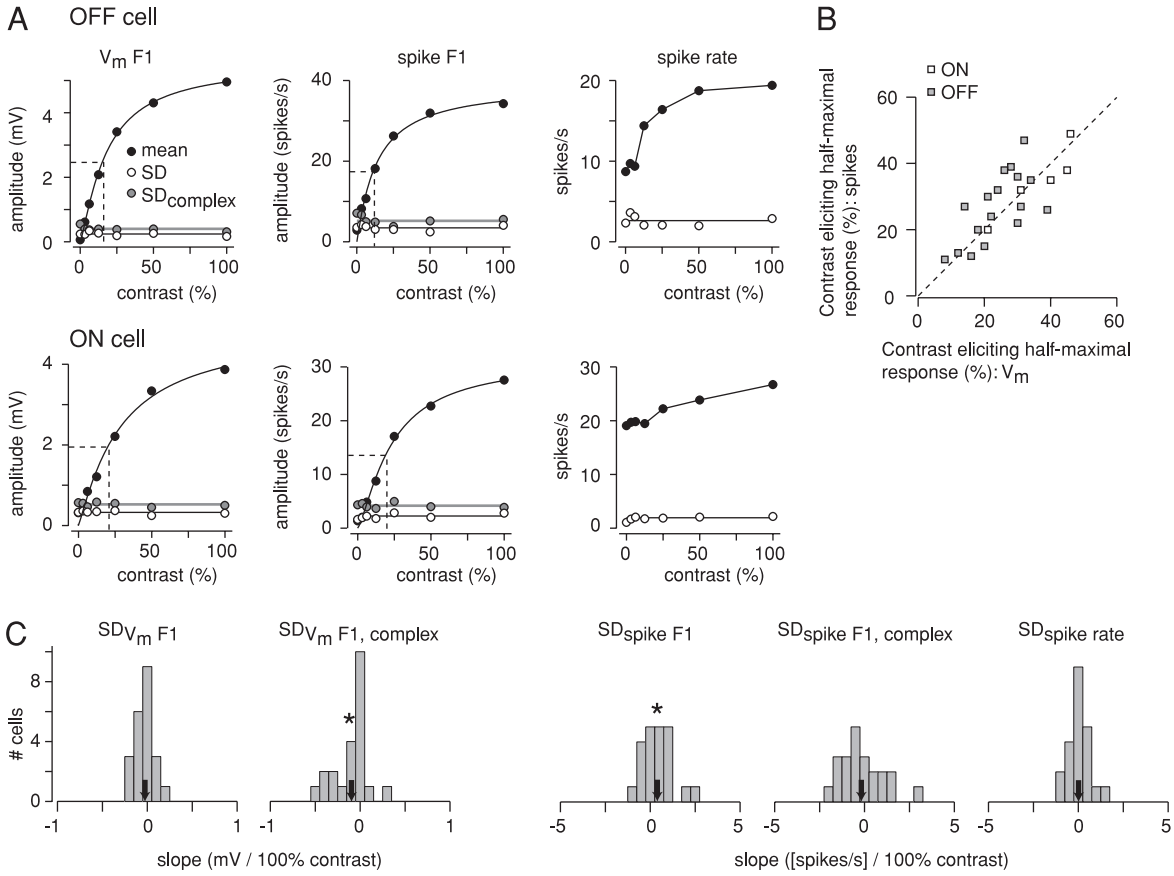

FIG. 2. Membrane potential and spiking responses increase with contrast but noise is constant. *A*: contrast response amplitudes for V_m and spikes at the stimulus fundamental frequency (F1), and spike rate all increased with contrast. F1 responses were fit with a descriptive function; - - -, contrast that elicited a half-maximal fitted response (see RESULTS). Noise, measured as the SD computed on amplitudes or in the complex plane, appeared flat for all measurements. OFF cell rested at −61 mV with a 9-Hz maintained discharge (12 repeats per contrast); ON cell rested at −61 mV with a 19-Hz maintained discharge (16 repeats per contrast). *B*: response functions reached half-maximal at similar contrast levels for spikes (29 ± 2.3%) and V_m (27 ± 2.2%). The correlation was $r = 0.75$ ($n = 22$, $P < 0.001$). *C*: histograms of slopes for noise vs. contrast. Slopes represent the change in V_m or spike rate over the full contrast range (0–100%). ↓, the mean of the distribution; *, a significant difference from a 0 slope for the population. $SD_{Vm\ F1,\ complex}$ was significantly <0 (–0.097 ± 0.041 mV/100% contrast, $P < 0.01$), and $SD_{spike\ F1}$ was significantly >0 (0.40 ± 0.18 Hz/100% contrast, $P < 0.05$. Both of these slopes were <2% of the maximum response amplitude (see RESULTS).

from zero (Fig. 2*C*). For $SD_{spike\ F1}$, the average slope increased by 0.40 ± 0.18 spikes/s from 0 to 100% contrast. This average slope was significantly greater than zero ($P < 0.05$) but represents <2% rise relative to the maximum spike F1 amplitude, 28.6 ± 2.0 spikes/s.

We measured the noise for the V_m as the SD of the F1, computed either on amplitudes ($SD_{Vm\ F1}$) or in the complex plane ($SD_{Vm\ F1,\ complex}$). Similar to the spikes, V_m F1 noise appeared to be constant as a function of contrast (Fig. 2*A*). On average, the slope of $SD_{Vm\ F1}$ was not different from zero (Fig. 2*C*). The $SD_{Vm\ F1,\ complex}$ showed a shallow negative slope of −0.097 ± 0.041 mV from 0 to 100% contrast, which is significantly below zero ($P < 0.01$) but represents <2% fall relative to the maximum V_m F1 amplitude, 5.5 ± 0.4 mV.

Across the five measures of noise, the two slight deviations from zero slope in the regression fits were on different SD measures ($SD_{spike\ F1}$ vs. $SD_{Vm\ F1,\ complex}$), were in different directions (slightly positive or negative), and were extremely small (<2%) relative to the range of signal amplitudes. Thus on all measures tested, noise was essentially independent of contrast.

Membrane fluctuations increase with contrast

We next measured fluctuations of V_m on a millisecond time scale (comparable to that of synaptic events). Because these fluctuations would be obscured by spikes, we blocked them by adding tetrodotoxin (TTX) to the bath. Then measuring contrast responses and their F1 noise, we found similar behavior to control conditions (compare Fig. 3*A* with Fig. 2*A*, *top*). Thus in the presence of TTX, the V_m response increased with contrast but the F1 noise ($SD_{Vm\ F1}$ or $SD_{Vm\ F1,\ complex}$) appeared constant.

To isolate fluctuations from the stimulus-driven response, we subtracted the "signal" from V_m to generate "fluctuation" traces. To measure fluctuation amplitude, we calculated the SD of the fluctuation traces at each time point (1 kHz) across cycles (see METHODS). As contrast modulated V_m, it also modulated the fluctuation amplitude. That is, fluctuations increased during the depolarizations that would normally lead to spiking (Fig. 3*A*).

Because TTX also blocks spikes in certain amacrine cells (e.g., Cook et al. 1998; Demb et al. 1999; Roska and Werblin 2003), whose direct synaptic input to the ganglion cell could

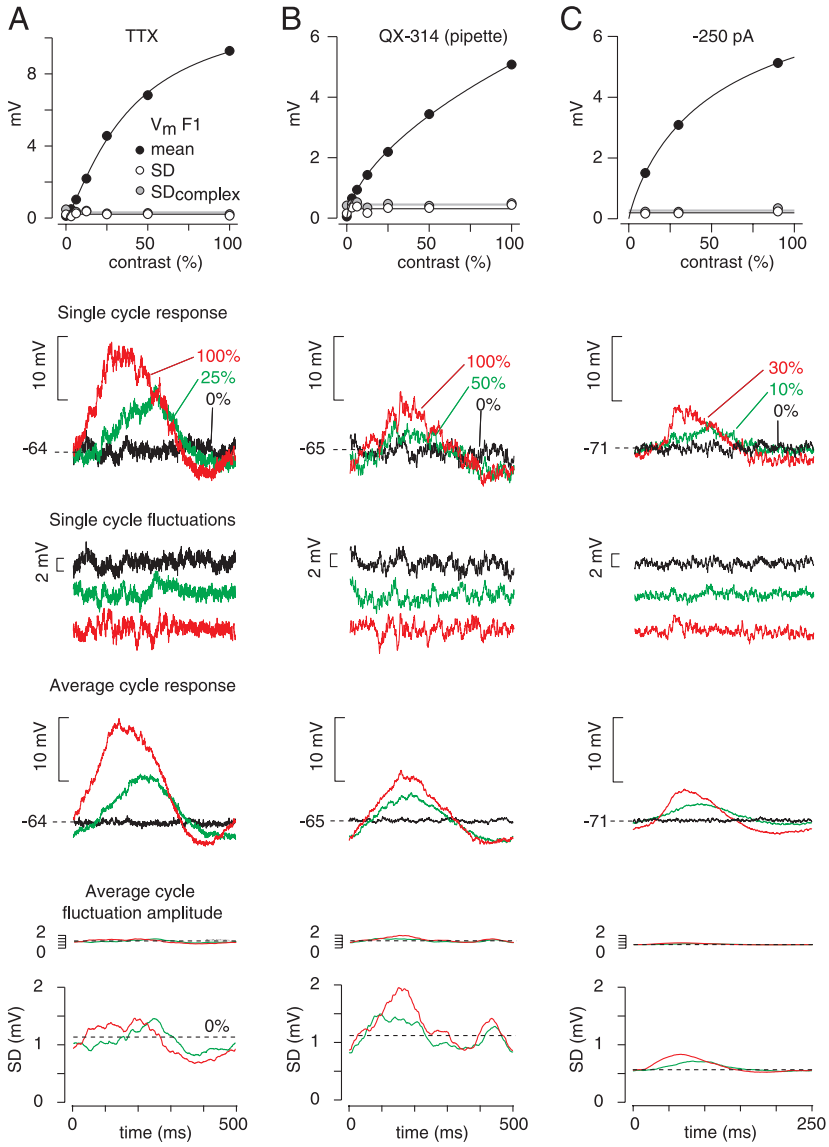

FIG. 3. Membrane fluctuations increase with contrast. *A*: spikes were blocked by applying TTX (100 nM) to the bath. *Top*: F1 amplitude increased with contrast, but noise (SD) appeared flat, similar to control conditions (same OFF cell as in Fig. 2*A*). *Second panel*: response across a single stimulus cycle at 3 contrasts. *Third panel*: fluctuations during single cycles at 3 contrasts; these are identical to the above traces with the mean and 1st 10 stimulus harmonics removed (see METHODS). Traces have been shifted vertically for display. *Fourth panel*: average response over 9 cycles. *Bottom*: average fluctuation amplitude over 9 cycles; this represents the SD of fluctuations (smoothed with a 50-ms window; see METHODS). Fluctuation amplitudes are shown both at the same scale as the average response and at an expanded scale. - - -, the average fluctuation amplitude at 0% contrast, which is expected to be constant. *B*: same as *A* except spikes were blocked by including QX-314 (50 mM) in the pipette (16 cycles; OFF cell). *C*: same as *A* except spikes were blocked by hyperpolarizing the cell with −250 pA steady current (50 cycles; OFF cell).

alter fluctuations, we took a second approach. We added QX-314 to the pipette solution to block sodium channels only in the recorded cell (Fig. 3*A*). As under TTX, fluctuations increased during the depolarization (Fig. 3*B*). However, under TTX, fluctuations typically decreased during hyperpolarization; whereas under QX-314 fluctuations sometimes increased during the hyperpolarization (Fig. 3*B*). This is probably because TTX blocks some amacrine cells that make inhibitory synapses on the ganglion cell that produce the hyperpolarization (Demb et al. 2001a,b). QX-314 leaves these inputs intact and thus allows the hyperpolarization and its accompanying fluctuations (Zaghloul et al. 2003). In a third approach, we hyperpolarized a cell with steady current (−150 or −250 pA) to eliminate spiking. This also revealed increased fluctuations during depolarization (Fig. 3*C*).

To test whether fluctuations reliably increased during depolarization, we performed a population analysis on 10 OFF cells with stable recordings while spikes were blocked (TTX, $n = 4$; QX-314, $n = 4$; hyperpolarizing current, $n = 2$). For each cell we measured the voltage at 0% contrast (i.e., resting potential at mean luminance) and the spontaneous fluctuation amplitude (SD of voltage across the full cycle; see METHODS). At various higher contrasts (1–9/cell), we measured the "peak response" as the voltage in a 50-ms window centered on the peak depolarization and the fluctuation amplitude as the SD of that voltage.

At zero stimulus contrast, the resting potential was −63.7 ± 4.0 mV and the spontaneous fluctuations had an amplitude (SD) of 0.84 ± 0.06 mV ($n = 10$ cells); this value includes noise in the recording system and thus serves as an upper limit on spontaneous fluctuation amplitude. At 9–12% contrast, cells depolarized from the resting potential by 2.2 ± 0.7 mV, and fluctuation amplitude increased to 1.0 ± 0.13 mV; the increase in fluctuation amplitude above baseline was 0.37 ± 0.19 mV ($n = 6$, $P < 0.10$) (the amplitude increase was calculated by taking the square-root of the difference between variances). At 25–30% contrast, cells depolarized 7.8 ± 1.9 mV, and fluctuation amplitude increased to 1.1 ± 0.07 mV, a significant increase above baseline by 0.71 ± 0.07 mV ($n = 8$, $P < 0.001$). At 100% contrast, cells depolarized by 11.7 ± 2.3 mV, and fluctuation amplitude increased to 1.3 ± 0.19 mV, a significant increase above baseline by 0.93 ± 0.18 mV ($n = 4$,

$P < 0.01$). Across all cells and contrasts, depolarizations from rest were as large as 17 mV, but the fluctuation increase above baseline was never more than 1.5 mV and was typically <1.0 mV (Fig. 4*A*). Thus membrane fluctuations become larger during depolarization, but the increased fluctuation amplitude remains small relative to the depolarization (<10% at high contrast).

We also analyzed the change in fluctuations during the most hyperpolarized 50-ms interval in the response ("trough response;" Fig. 4*B*). In some recordings (bath-applied TTX), the trough response was positive to the resting potential, and here the fluctuation amplitude was also above the spontaneous level. But in most cases, the trough response was below the resting potential, and there was a slight decrease in fluctuation amplitude below spontaneous levels (by ~0.4 mV; Fig. 4*B*).

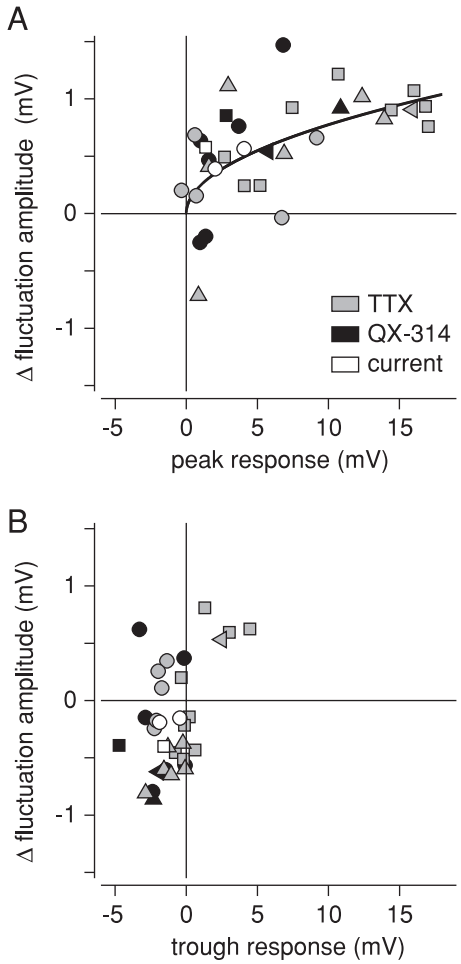

FIG. 4. As a cell depolarizes membrane fluctuations increase in amplitude. *A*: the depolarization amplitude above the resting potential (peak response) is plotted against the change in fluctuation amplitude relative to the spontaneous fluctuation amplitude, 0.84 ± 0.06 mV (Δ fluctuation amplitude); Δ fluctuation amplitude was calculated by taking the square-root of the difference between variances. Responses of 10 cells (different symbols) to different contrast levels; shading of points indicates condition used to block spiking (TTX, $n = 4$; QX-314 pipette, $n = 4$; hyperpolarizing current, $n = 2$). The response and fluctuation amplitudes were both averaged over a 50-ms window around the peak of the depolarization. In general, Δ fluctuation amplitude increased with response, but was small (always <1.5 mV; usually <1.0 mV) relative to the response (≤17 mV). The line (fitted by eye) shows an approximate relationship between Δ fluctuation amplitude and response: Δ fluctuation amplitude = $(0.06 \text{ response})^{0.5}$. The 0.06 factor is ≪1 because of the nature of the elementary synaptic events, which are approximately decreasing exponentials with a small peak amplitude (Freed 2000a). *B*: the amplitude of the most hyperpolarized response in the stimulus cycle relative to the resting potential (trough response) is plotted against Δ fluctuation. Symbols are the same format as *A*. The trough response was typically a small hyperpolarization accompanied by a small decrease in fluctuation amplitude (on average, by ~0.4 mV).

Model captures the main features of the V_m response

To understand how noise in a ganglion cell's F1 response can remain constant with contrast (Figs. 2 and 3) despite increased fluctuations (Figs. 3 and 4), we used a simple model to represent a ganglion cell with converging excitatory synapses (see METHODS). Each bipolar synapse was simulated as a series of excitatory postsynaptic potentials (EPSPs) that rose fast and decayed exponentially. The average rate was modulated, but the timing of individual EPSPs followed Poisson statistics (Freed 2000a). Parameter values were based on previous measurements (see METHODS): 1,000 synapses; EPSP amplitude, 0.1 mV; EPSP decay constant (τ), 10 ms; basal rate, 4 EPSPs synapse^{-1} s^{-1} (Freed 2000a,b). A contrast signal was modeled as the basal rate plus a sinusoidally modulated rate, 1–4 EPSPs synapse^{-1} s^{-1}.

The voltage response behaved like the measured response in real cells (Fig. 5*A*), and we quantified it in the same way. The model's F1 response increased with contrast while its F1 noise was independent of contrast (Fig. 5*C*, *top*). Fluctuation amplitude (SD) at mean luminance was 0.45 mV, and during a peak depolarization of 3.9 mV, the fluctuation amplitude increased to 0.63, an increase of 0.44 mV (Fig. 5*C*; the amplitude increase was calculated by taking the square-root of the difference between variances). Thus just as for real data, the F1 noise was steady with contrast, but the fluctuation amplitude during the depolarization increased with contrast.

That membrane fluctuations increased with contrast was expected from the Poisson statistics of EPSP arrival times. That the F1 noise was steady with contrast was also expected because the noise increase during the depolarizing half-cycle essentially canceled the noise decrease during the hyperpolarizing half-cycle. Furthermore, the model, similar to real cells, produced a relatively small change in fluctuation amplitude relative to the peak depolarization.

Low EPSP rates and short time constants cause noise to increase with contrast

To create a model where noise *does* increase significantly with response, we changed certain parameters. First, we eliminated the basal EPSP rate (Fig. 5*C*). Here, the rise in fluctuation amplitude becomes larger relative to the response modulation. Furthermore, there was a slight increase in F1 noise with response level (Fig. 5*C*, *top*) because increasing depolarization was accompanied by increased fluctuation amplitude (Fig. 5*C*, *middle* and *bottom*), but this increase is no longer canceled by a decrease during the hyperpolarizing half-cycle.

Next, we reduced the number of synapses by 10-fold but maintained the same average response level by increasing EPSP amplitude by the same factor. Conceptually, this test is identical to the previous one except that release within each bundle of 10 synapses is fully correlated. Thus the total EPSP response arises from only 100 independent bundles. Here, the rise in fluctuation amplitude began to approach the scale of the F1 modulation (Fig. 5*C*). The impact of these fluctuations can

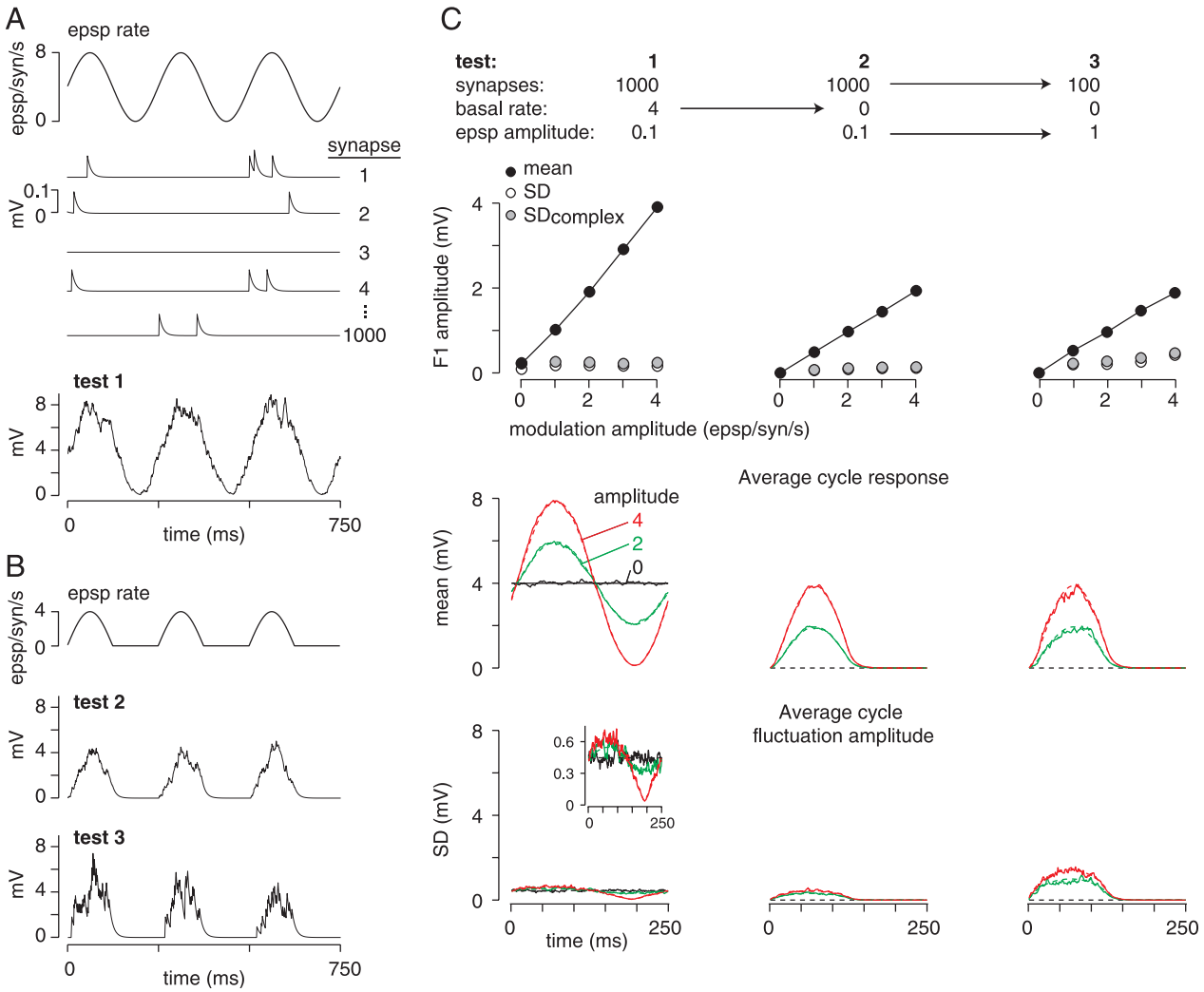

FIG. 5. Contrast-dependent change in membrane fluctuations is effectively attenuated by synaptic convergence. *A*: the model, *test 1*: each synapse produced excitatory postsynaptic potentials (EPSPs) according to a Poisson-modulated release rate. An EPSP was modeled as an exponential (peak amplitude, 0.1 mV; time constant, 10 ms). The voltage trace of *test 1* summed 1, 000 synapses (3 cycles of 50 shown; 4-Hz modulation). *B*: for *tests 2* and *3*, release rate was rectified (i.e., 0 release rate at baseline). *Test 2* had 1,000 synapses and *test 3* had only 100 (EPSP amplitude, 1 mV). *C, top*: F1 amplitude vs. the peak amplitude of synaptic release above baseline (expressed as epsps synapse^{-1} s^{-1}); this is analogous to the contrast response functions for V_m in Figs. 2 and 3. *Middle* and *bottom*: average cycle mean response and fluctuation amplitude for 3 levels of release rate (—); these are analogous to the *bottom 2 rows* in Fig. 3. *Inset* (*bottom row* for *test 1*): an expanded vertical axis. - - -, the expected values of mean response and noise calculated from equations (see METHODS).

be appreciated by examining the raw trace of *test 3* (Fig. 5*B*). Furthermore, this caused a clear rise in F1 noise with response level (Fig. 5*C*).

We ran 24 tests that fully evaluated the following parameters: number of synapses (100, 1,000); EPSP τ (5, 10, 20 ms); basal release rate (0, 1, 2, 4 EPSPs synapse^{-1} s^{-1}). A modulated EPSP rate was added to the basal rate (1–4 EPSPs synapse^{-1} s^{-1}). In general, the increase in fluctuation amplitude was maximal when the basal rate was low, the number of synapses was low, and the EPSP τ was short. The F1 noise rose most steeply with modulation amplitude when the basal release rate was low and the number of synapses was low.

Spike responses precede V_m responses, further minimizing the impact of V_m fluctuations

The peak spiking response occurred during the rise in V_m and thus preceded the peak membrane response. The relatively early peak in the spiking response can be quantified as an advance in the response phase relative to the V_m response (Fig. 6). Across all cells, the phase advance at high contrast was 35.6 ± 1.6°. Thus when fluctuation amplitude peaked, the spike response was already on the decline (Fig. 6).

DISCUSSION

This study addresses an important paradox. As stronger stimuli increase the release rate of excitatory transmitter vesicles onto a large ganglion cell, the Poisson nature of synaptic release causes increased fluctuations of the membrane potential (proportional to the square root of the mean quantal rate) (Freed 2000a,b) (Figs. 3 and 4). However, this contrast-*dependent* rise in fluctuation amplitude is not reflected in the F1 amplitude of the V_m or the spikes (Figs. 2 and 3); contrast-*dependent* noise is also absent from the spike rate (Croner et al.

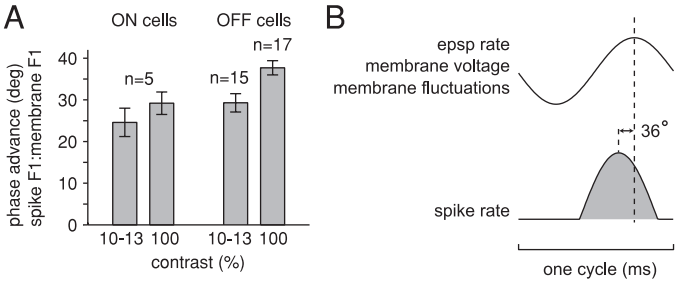

FIG. 6. Phase shift between V_m and spike rate minimizes the impact of membrane fluctuations on spiking. *A*: the F1 phase of the spike response was advanced relative to the F1 phase of the membrane response, for both ON and OFF cells at both low and high contrast. *B*: sinusoidal modulation of EPSP's causes sinusoidal modulation of ganglion cell membrane voltage and fluctuation amplitude. The spike response (shown as a rectified sine-wave) peaks ~36° before peak membrane voltage and thus earlier than the peak in membrane fluctuation amplitude (see RESULTS). Consequently membrane fluctuations peak when spike rate is declining, minimizing their impact on spiking.

1993; Reich et al. 1997; Rüttiger et al. 2002; Sestokas and Lehmkuhle 1988; Sun et al. 2004) (Fig. 2).

The resolution now seems simple: the stimulus-driven change in fluctuation amplitude is ~10-fold smaller than the depolarization (Figs. 3 and 4), and so the slow (F1) modulation provides the dominant drive toward spike threshold. The relatively small amplitude of fluctuations arises partially from the integration of synaptic events with Poisson arrival times combined with the (approximately) exponential shape of an event, which yields a variance:mean ratio $\ll 1$ (Katz and Miledi 1972). Small fluctuations also arise from a large number of synaptic inputs (approximately thousands per second) and a typically short EPSP time constant (τ, ~10 ms; Fig. 5). These last two factors can be understood by considering the signal: noise ratio (V/σ), calculated from the steady-state equations (see METHODS), which simplifies to $(2\,n\,\tau)^{0.5}$ (where n is number of synaptic events = number of synapses × release rate synapse^{-1}). Thus signal:noise improves with large n and long τ.

Finally, when fluctuation amplitude is largest (peak of the membrane depolarization), the spike response is already declining (Fig. 6). That peak spike rate precedes the peak depolarization may arise because spikes are driven partly by dV/dt and because sodium channels inactivate during the peak depolarization, especially at low temporal frequencies (~2 Hz). Thus the nature of synaptic inputs (number and time constant) and the nature of spike generation cooperate to prevent contrast-dependent increases in fluctuation amplitudes from causing contrast-dependent increases in spike noise.

Contrast-independent noise in the F1 response

Constant, contrast-*independent* noise in the V_m F1 amplitude was found in real cells and in the model (Figs. 2, 3, and 5). For the model, fluctuation amplitude increases during the depolarization and decreases during the hyperpolarization apparently cancel one another, and consequently, F1 noise in the V_m is effectively independent of contrast (*test 1* of the model; Fig. 5). Contrast-dependent fluctuations contribute noticeably to the membrane F1 modulation only when basal release and the number of independent synaptic inputs are both low (*test 3* of the model; Fig. 5). For most real cells, there was an increased fluctuation amplitude during the depolarization that was partially cancelled by a decreased amplitude during the hyperpolarization (Figs. 3 and 4). But perhaps more significantly, changes in fluctuation amplitude were relatively small compared with the amplitude of the F1 modulation (Figs. 3 and 4). Consequently, F1 noise in the V_m was effectively independent of contrast (Figs. 2 and 3).

We used periodic stimuli to allow direct comparison to previous in vivo studies. With these stimuli, the meaning of F1 signal and noise is clear. However, for more natural stimuli that contain multiple temporal frequencies, spike responses arrive in "bursts" (Meister and Berry 1999; Reinagel 2001; Reinagel and Reid 2000; van Hateren et al. 2002). Thus the findings regarding F1 signal and noise are difficult to extend to these more natural conditions. However, the relatively small change in fluctuation amplitude represents a fundamental property that should generalize to most stimulus-response relationships (i.e., responses to nonperiodic stimuli).

Model predictions for other cell types and eccentricity

One important strategy for minimizing fluctuation amplitudes is to integrate a large number of synaptic events (i.e., number of synapses × release rate synapse^{-1}). This strategy will work for small ganglion cells that integrate $\ll$1,000 synapses only if the release rate at each synapse is substantially increased to offset the small number of synapses. For example, the small, brisk-sustained (beta) ganglion cell of cat central retina receives, not 1,000 synapses like an alpha cell, but ~150. Furthermore, a beta cell's synapses are probably not completely independent because they arise from relatively few bipolar cells, some of which contribute >30 contacts to a given cell (Cohen and Sterling 1992). Similarly, the P (midget) ganglion cell of primate central retina receives ~50 ribbon synapses, all probably correlated because they arise from a single midget bipolar cell (Calkins et al. 1994). And yet these small cells show the same noise properties in their spiking response as large ganglion cells in the periphery (Croner et al. 1993; Rüttiger et al. 2002; Sestokas and Lehmkuhle 1988). For small cells to show similar behavior as large cells in our model, high release rates (EPSPs · synapse^{-1} · s^{-1}) would have to offset the low number of independent synapses. For example, *test 1* of the model used 1,000 synapses with a rate that ranged from 0 to 8 EPSPs · synapse^{-1} · s^{-1}, but an identical model could use 10-fold fewer synapses (100) with a 10-fold higher rate (0–80 EPSPs · synapse^{-1} · s^{-1}).

There is in fact evidence that bipolar inputs to small ganglion cells provide relatively high rates of release. Two types of "sustained" bipolar cell in cat retina (b_2 and b_3), which contribute half of the beta cell's ribbon input, apparently release ~50 quanta/s at steady photopic luminance (Cohen and Sterling 1992; Freed 2000b). By comparison, the "transient" bipolar cell that provides most ribbon synapses to the alpha cell apparently has a lower rate of ~2 quanta/s (Freed 2000a,b; Freed and Sterling 1988). The midget cell's brisk-sustained response resembles the beta cell's, suggesting that its midget bipolar cell might also show substantial basal release. The model suggests that beyond the central retina, as dendritic fields expand and collect more synapses in smaller bundles, the bipolar cells can relax their release rates without causing significant contrast-dependent noise in the spike output.

Limitations of the model

In capturing the main findings with the simplest architecture (Shadlen and Newsome 1994), we used a constant EPSP shape and amplitude; whereas in reality these vary (Bekkers et al. 1990; Frerking and Wilson 1996) and could increase fluctuations in the model response by 25% (Freed 2000a; Taylor et al. 1995). Furthermore, EPSP amplitudes would be reduced at depolarized potentials due to reduced driving force. However, given the resting potential (−65 mV), the likely EPSP reversal potential (0 mV), and the typical response deviation from baseline (±6 mV), this factor should affect EPSP amplitude by <10%.

The model omitted voltage-gated channels. Although these would certainly contribute to fluctuation amplitudes, the dominant contribution seems to be synaptic excitation (van Rossum et al. 2003). Evidence for dominant synaptic excitation comes from blocking ON bipolar synaptic input to a ganglion cell with L-2-amino-4-phosphonobutyric acid (L-AP-4), which considerably reduces ganglion cell fluctuations (e.g., Freed 2000a; Zaghloul et al. 2003). The model also omitted inhibition even though the alpha cell certainly receives "feedforward" inhibition during the depolarizing response (Flores-Herr et al. 2001; Pang et al. 2002; Roska and Weblin 2001; Zaghloul et al. 2003), and numerous inhibitory synapses that comprise ~80% of its contacts (Freed and Sterling 1988; Kolb and Nelson 1993; Weber and Stanford 1994). However, given the relatively long inhibitory postsynaptic potential (IPSP) time constant ($\tau \gg 10$ ms) (Tian et al. 1998; Freed et al. 2003) and the potentially high rate of release (n), the signal:noise ratio $[(2\ n\ \tau)^{0.5}]$ for inhibitory inputs should be high. Probably as a consequence, IPSPs are found to add little noise (Freed 2000a). Finally, we omitted the spike generator, but this would not affect our conclusions because, like the model, real cells show the basic phenomena with spikes blocked (Fig. 3).

Why do retina and cortex differ?

An OFF alpha ganglion cell in retina and a pyramidal cell in primary visual cortex share certain properties. They are comparable in size, with thickish, longish dendrites and ≥1,000 excitatory inputs (Braitenberg and Schüz 1998; Freed and Sterling 1988; Kier et al. 1995; Shadlen and Newsome 1994, 1998); and both have a low maintained discharge (~5 spikes/s) so that spike responses resemble "bursts." However, noise in the ganglion cell spike rate was clearly contrast-*independent* (Fig. 2); whereas noise in many cortical cells, stimulated and analyzed similarly, is clearly contrast-*dependent* (Dean 1981; Tolhurst et al. 1981 1983). One exception may be cortical cells in the input layer, where noise is apparently relatively low (Kara et al. 2000). Another exception may be cortical cells recorded in awake animals where noise may be independent of contrast, similar to the retina (after excluding effects of eye movements) (Gur et al. 1997). Clearly, our model can explain only the behavior of ganglion cells and potentially a subset of cortical cells (Fig. 5, *test 1* of the model).

Perhaps noise in an individual cell represents a much greater concern in the retina than the cortex. In retina, each point in the visual field is represented by approximately one ganglion cell of a given type (DeVries and Baylor 1997), and so here it may be critical to transfer a signal with low noise. Of course there is a cost: a high rate of bipolar cell synaptic release, which requires energy (Attwell and Laughlin 2001). In cortex, where the same point in visual space is represented by more than ~100 cells, coding may be distributed across the population. This would relax the requirement for low noise in a single cell and thus save the cost of high release rates. One alternative to this proposal is that V_m fluctuations in the cortex are in some way beneficial, for example, by smoothing the relationship between subthreshold V_m and spiking responses (Anderson et al. 2000).

ACKNOWLEDGMENTS

We thank C. Passaglia and R. Smith for comments on the manuscript.

GRANTS

This work was supported by National Eye Institute Grants F32-EY-06850 to J. B. Demb, EY-00828 to P. Sterling, and EY-13333 to M. A. Freed.

REFERENCES

Anderson JS, Lampl I, Gillespie DC, and Ferster D. The contribution of noise to contrast invariance of orientation tuning in cat visual cortex. *Science* 290: 1968–1972, 2000.

Attwell D and Laughlin SB. An energy budget for signaling in the grey matter of the brain. *J Cereb Blood Flow Metab* 21: 1133–1145, 2001.

Bekkers JM, Richerson GB, and Stevens CF. Origin of variability in quantal size in cultured hippocampal neurons and hippocampal slices. *Proc Natl Acad Sci USA* 87: 5359–5362, 1990.

Brainard DH. The psychophysics toolbox. *Spat Vis* 10: 433–436, 1997.

Braitenberg V and Schüz A. *Cortex: Statistics and Geometry of Neuronal Connectivity*. New York: Springer-Verlag, 1998.

Calkins DJ, Schein SJ, Tsukamoto Y, and Sterling P. M and L cones in macaque fovea connect to midget ganglion cells by different numbers of excitatory synapses. *Nature* 371: 70–72, 1994.

Cohen E and Sterling P. Parallel circuits from cones to the on-beta ganglion cell. *Eur J Neurosci* 4: 506–520, 1992.

Cook PB, Lukasiewicz PD, and McReynolds JS. Action potentials are required for the lateral transmission of glycinergic transient inhibition in the amphibian retina. *J Neurosci* 18: 2301–2308, 1998.

Croner LJ, Purpura K, and Kaplan E. Response variability in retinal ganglion cells of primates. *Proc Natl Acad Sci USA* 90: 8128–8130, 1993.

Dean AF. The variability of discharge of simple cells in the cat striate cortex. *Exp Brain Res* 44: 437–440, 1981.

Demb JB, Haarsma L, Freed MA, and Sterling P. Functional circuitry of the retinal ganglion cell's nonlinear receptive field. *J Neurosci* 19: 9756–9767, 1999.

Demb JB, Zaghloul K, Haarsma L, and Sterling P. Bipolar cells contribute to nonlinear spatial summation in the brisk-transient (Y) ganglion cell inmammalian retina. *J Neurosci* 21: 7447–54, 2001a.

Demb JB, Zaghloul K, and Sterling P. Cellular basis for the response to second-order motion cues in Y retinal ganglion cells. *Neuron* 20: 711–21, 2001b.

Devries SH and Baylor DA. Mosaic arrangement of ganglion cell receptive fields in rabbit retina. *J Neurophysiol* 78: 2048–2060, 1997.

Enroth-Cugell C and Robson JG. The contrast sensitivity of retinal ganglion cells of the cat. *J Physiol* 187: 517–552, 1966.

Flores-Herr N, Protti DA, and Wassle H. Synaptic currents generating the inhibitory surround of ganglion cells in the mammalian retina. *J Neurosci* 21: 4852–4863, 2001.

Freed MA. Rate of quantal excitation to a retinal ganglion cell evoked by sensory input. *J Neurophysiol* 83: 2956–2966, 2000a.

Freed MA. Parallel cone bipolar pathways to a ganglion cell use different rates and amplitudes of quantal excitation. *J Neurosci* 20: 3956–3963, 2000b.

Freed MA, Smith RG, and Sterling P. Timing of quantal release from the retinal bipolar terminal is regulated by a feedback circuit. *Neuron* 38: 89–101, 2003.

Freed MA and Sterling P. The ON-alpha ganglion cell of the cat retina and its presynaptic cell types. *J Neurosci* 8: 2303–2320, 1988.

Frerking M and Wilson M. Effects of variance in mini amplitude on stimulus-evoked release: a comparison of two models. *Biophys J* 70: 2078–2091, 1996.

Gur M, Beylin A, and Snodderly DM. Response variability of neurons in primary visual cortex (V1) of alert monkeys. *J Neurosci* 17: 2914–2920, 1997.

Hochstein S and Shapley RM. Linear and nonlinear spatial subunits in Y cat retinal ganglion cells. *J Physiol* 262: 265–284, 1976.

Kara P, Reinagel P, and Reid RC. Low response variability in simultaneously recorded retinal, thalamic, and cortical neurons. *Neuron* 27: 635–646, 2000.

Katz B and Miledi R. The statistical nature of the acetycholine potential and its molecular components. *J Physiol* 224: 665–699, 1972.

Kier CK, Buchsbaum G, and Sterling P. How retinal microcircuits scale for ganglion cells of different size. *J Neurosci* 15: 7673–7683, 1995.

Kolb H and Nelson R. OFF-alpha and OFF-beta ganglion cells in cat retina. II. Neural circuitry as revealed by electron microscopy of HRP stains. *J Comp Neurol* 329: 85–110, 1993.

Laughlin SB, Howard J, and Blakeslee B. Synaptic limitations to contrast coding in the retina of the blowfly *Calliphora*. *Proc R Soc Lond B Biol Sci* 231: 437–467, 1987.

Laughlin SB and Sejnowski TJ. Communication in neuronal networks. *Science* 301: 1870–1874, 2003.

Levine MW, Cleland BG, and Zimmerman RP. Variability of responses of cat retinal ganglion cells. *Vis Neurosci* 8: 277–279, 1992.

Levine MW, Cleland BG, Mukherjee P, and Kaplan E. Tailoring of variability in the lateral geniculate nucleus of the cat. *Biol Cybern* 75: 219–227, 1996.

Meister M and Berry MJ 2nd. The neural code of the retina. *Neuron* 22: 435–450, 1999.

Naka KI and Rushton WA. S-potentials from color units in the retina of fish (*Cyprinidae*). *J Physiol* 185: 536–555, 1966.

Pang JJ, Gao F, and Wu SM. Relative contributions of bipolar cell and amacrine cell inputs to light responses of ON, OFF, and ON-OFF retinal ganglion cells. *Vision Res* 42: 19–27, 2002.

Peichl L, Ott H, and Boycott BB. Alpha ganglion cells in mammalian retinae. *Proc R Soc Lond B Biol Sci* 231: 169–197, 1987.

Pelli DG. The VideoToolbox software for visual psychophysics: transforming numbers into movies. *Spat Vis* 10: 437–442, 1997.

Reich DS, Victor JD, Knight BW, Ozaki T, and Kaplan E. Response variability and timing precision of neuronal spike trains in vivo. *J Neurophysiol* 77: 2836–2841, 1997.

Reinagel P. How do visual neurons respond in the real world? *Curr Opin Neurobiol* 11: 437–42, 2001.

Reinagel P and Reid RC. Temporal coding of visual information in the thalamus. *J Neurosci* 20: 5392–400, 2000.

Rice SO. Mathematical analysis of random noise. *Bell Syst Tech J* 23: 282–332, 1944.

Roska B and Werblin F. Vertical interactions across 10 parallel, stacked representations in the mammalian retina. *Nature* 410: 583–587, 2001.

Roska B and Werblin F. Rapid global shifts in natural scenes block spiking in specific ganglion cell types. *Nat Neurosci* 6: 600–608, 2003.

Rüttiger L, Lee B, and Sun H. Transient cells can be neurometrically sustained: the positional accuracy or retinal signals to moving targets. *J Vis* 2: 232–242, 2002.

Schiller PH, Finlay BL, and Volman SF. Short-term response variability of monkey striate neurons. *Brain Res* 105: 347–349, 1976.

Segal JR, Ceccarelli B, Fesce R, and Hurlbut WP. Miniature endplate potential frequency and amplitude determined by an extension of Campbell's theorem. *Biophys J* 47: 183–202, 1985.

Sestokas AK and Lehmkuhle S. Response variability of X- and Y-cells in the dorsal lateral geniculate nucleus of the cat. *J Neurophysiol* 59: 317–325, 1988.

Shadlen MN and Newsome WT. Noise, neural codes and cortical organization. *Curr Opin Neurobiol* 4: 569–579, 1994.

Shadlen MN and Newsome WT. The variable discharge of cortical neurons: implications for connectivity, computation, and information coding. *J Neurosci* 18: 3870–3896, 1998.

Sun H, Rüttiger L, and Lee BB. The spatiotemporal precision of ganglion cell signals: a comparison of physiological and psychophysical performance with moving gratings. *Vision Res* 44: 19–33, 2004.

Taylor WR, Chen E, and Copenhagen DR. Characterization of spontaneous excitatory synaptic currents in salamander retinal ganglion cells. *J Physiol* 486: 207–221, 1995.

Tian N, Hwang TN, and Copenhagen DR. Analysis of excitatory and inhibitory spontaneous synaptic activity in mouse retinal ganglion cells. *J Neurophysiol* 80: 1327–1340, 1998.

Tolhurst DJ, Movshon JA, and Thompson ID. The dependence of response amplitude and variance of cat visual cortical neurons on stimulus contrast. *Exp Brain Res* 41: 414–419, 1981.

Tolhurst DJ, Movshon JA, and Dean AF. The statistical reliability of signals in single neurons in cat and monkey visual cortex. *Vision Res* 23: 775–785, 1983.

Troy JB and Robson JG. Steady discharges of X and Y retinal ganglion cells of cat under photopic illuminance. *Vis Neurosci* 9: 535–553, 1992.

van Hateren JH, Ruttiger L, Sun H, and Lee BB. Processing of natural temporal stimuli by macaque retinal ganglion cells. *J Neurosci* 22: 9945–60, 2002.

van Rossum MC, O'Brien BJ, and Smith RG. Effects of noise on the spike timing precision of retinal ganglion cells. *J Neurophysiol* 89: 2406–2419, 2003.

Weber AJ and Stanford LR. Synaptology of physiologically identified ganglion cells in the cat retina: a comparison of retinal X- and Y-cells. *J Comp Neurol* 343: 483–499, 1994.

Zaghloul KA, Boahen K, and Demb JB. Different circuits for ON and OFF retinal ganglion cells cause different contrast sensitivities. *J Neurosci* 23: 2645–2654, 2003.